Multiwavelength Thermal Lens Spectrophotometer Based on an Acousto-Optic Tunable Filter

Chieu D. Tran* and Valerian Simianu

Department of Chemistry, Marquette University, Milwaukee, Wisconsin 53233

The instrumentation development of a novel, all solid-state, nonmoving parts, fast-scanning and wide-tuning range multiwavelength thermal lens spectrophotometer based on the acousto-optic tunable filter (AOTF) is described. Initially, the essential electronic driver was developed to facilitate the systematic characterization of the paratellurite (TeO_2) AOTF and to demonstrate that this filter can be successfully and uniquely used as an all solid-state, nonmoving parts dispersive device to rapidly diffract white incident light into a selected color beam, to amplitude modulate the diffracted monochromatic light, and to keep its intensity constant. The multiwavelength thermal lens instrument was subsequently constructed using this AOTF, and preliminary results on advantages of this spectrophotometer such as its ability to characterize trace chemicals and to analyze multicomponent samples are delineated.

INTRODUCTION

Thermal lens techniques have been demonstrated to be sensitive methods for low-absorbance measurements. They can be used for the determination of absorptivities as low as 10^{-7}.[1-5] However, in spite of their advantages such as noncontacting, in situ capability, precision, sensitivity, expanded dynamic range, and minimal sample requirements they are still relatively underutilized compared with other spectrochemical methods. The lack of selectivity is probably the main reason for this limited use. In fact, the majority of published thermal lens techniques have employed only one excitation wavelength, and the use of only a single wavelength severely hinders the use of these promising techniques for the identification of unknown samples as well as for the analysis of mixtures of compounds.[1-5]

Our recent effort is focused on the development of a novel instrument which has higher selectivity than the conventional thermal lens instruments. We have developed a novel dual wavelength thermal lens spectrophotometer that is capable of simultaneously measuring the thermal lens signals at two different wavelengths.[6-9] The dual wavelength capability enables this spectrometer to be used for the identification of samples, the detection of two component mixtures, and the determination of the pHs of solutions at very low indicator concentrations.[6-9]

It is thus clear that the use of multiwavelength excitation techniques introduces much needed selectivity into the thermal lens techniques.[6-9] The induced selectivity is expected to be directly proportional to the number of excitation wavelengths. The greater the number of excitation wavelengths employed, the higher the selectivity is. In fact, we have demonstrated recently that samples which have up to four different components can be quantitatively determined in one measurement without any pretreatment, by use of the four wavelength thermal lens spectrophotometer.[10] Obviously, more optical components such as mirrors and beamsplitters were needed as the number of excitation wavelengths increased.[10] This in turn made the instrument complex and prone to vibrations, interferences. This increased complexity can be readily ameliorated with the use of the recently developed acousto-optic tunable filter.

Acousto-optic tunable filter (AOTF) is a solid-state electronically tunable spectral band-pass filter which operates on the principle of acousto-optic interaction in an anisotropic medium.[11-16] Generally, the AOTF is constructed from such birefringent crystal as TeO_2 onto which an array of piezoelectric transducers is bonded.[11-16] Acoustic waves are generated and launched into the crystal when a rf signal is applied into these transducers. These propagating acoustic waves produce a periodic moving grating which will diffract portions of an incident light beam. A light beam propagating as an extraordinary ray (e-ray) can, under some conditions, be converted into an ordinary ray (o-ray) and, in addition, be spatially separated from the original e-ray by interaction with, and diffraction from, an acoustic wave propagating in the AOTF. Since the polarization of the incident and the diffracted beam are different, the corresponding refractive indices are different. As a consequence, for a fixed acoustic frequency only a very narrow band of optical frequencies can approximately satisfy the phase matching condition or the conservation of momentum (i.e., $\vec{k}_d = \vec{k}_i + \vec{k}_s$ where $\vec{k}_i$, $\vec{k}_d$, and $\vec{k}_s$ are the wave vectors of the incident and diffrated light and of the acoustic wave, respectively) and be diffracted. The spectral band pass of the filter can, therefore, be tuned over large optical regions by changing the frequency of the applied radio frequency (rf) signal (and thus change $\vec{k}_s$). The AOTF is thus similar to the diffraction grating. One of the obvious advantages of the AOTF is that its grating constant, which in this case is the frequency of the acoustic wave, can be electronically changed. Rapid scanning of the filter is therefore possible. In fact, since the scanning speed of the AOTF is controlled by the transit time of an acoustic wave across an optial beam which is on the order of a few microseconds, the tuning speed of the filter can be very fast. Therefore, compared to other dispersive devices, AOTF has such advantages as (1) compact, all solid-state, rugged, and contains no moving parts; (2) wide angular field; (3) wide tuning range (from UV through visible to IR); (4) high spectral

(1) Kliger, D. S. *Ultrasensitive Laser Spectroscopy*; Academic: New York, 1983.
(2) Harris, J. M.; Dovichi, N. J. *Anal. Chem.* **1980**, *52*, 695A.
(3) Teramae, N.; Winefordner, J. D. *Appl. Spectrosc.* **1987**, *41*, 164.
(4) Tran, C. D. *Anal. Chem.* **1980**, *60*, 182.
(5) Tran, C. D.; Van Fleet, T. A. *Anal. Chem.* **1988**, *60*, 2478.
(6) Franko, M.; Tran, C. D. *Anal. Chem.* **1988**, *60*, 1925.
(7) Tran, C. D.; Franko, M. *J. Phys. E: Sci. Instrum.* **1989**, *22*, 586.
(8) Franko, M.; Tran, C. D. *Appl. Spectrosc.* **1989**, *43*, 661.
(9) Tran, C. D.; Xu, M. *Appl. Spectrosc.* **1989**, *43*, 1056.
(10) Xu, M.; Tran, C. D. *Anal. Chim. Acta* **1990**, *235*, 445.
(11) Yano, T.; Watanabe, A. *Appl. Opt.* **1976**, *15*, 2250.
(12) Chang, I. C. *SPIE Acousto-Optics* **1976**, *90*, 12.
(13) Chang, I. C. *Opt. Eng.* **1981**, *20*, 824.
(14) Sivanayayam, A.; Findley, D. *Appl. Opt.* **1984**, *23*, 4601.
(15) Shipp, W. S.; Biggins, J.; Wade, C. W. *Rev. Sci. Instrum.* **1976**, *47*, 565.
(16) Nelson, R. L. *Instrum. Soc. Am. Trans.* **1986**, *25*, 31.

0003-2700/92/0364-1419$03.00/0

resolution (bandwidth of light transmitted by the filter is about 2–6 Å); (5) rapid scanning ability (order of a few microseconds); (6) high-speed random or sequential wavelength access; and (7) imaging capability. Consequently, AOTF has been called "the new generation monochromator" and has provided a unique means for the development of novel instruments which range from the fast-scanning UV, visible, and IR spectrophotometers to the astronomical photometer, multigas analyzer, and the fluorescence microscopy.[11-19] It should be noted that fast-scanning ability is the only advantage of the AOTF that was exploited in these instruments. As a consequence, to date, the stability of the AOTF in terms of spectra and intensity has not been assessed. Furthermore, it is interesting to point out that in spite of its potentials, to date, the AOTF has not been incorporated into any multiwavelength laser-based instrument. This is rather unfortunate because the synergistic use of the laser and the AOTF should make the AOTF-based thermal lens instrument have all the combined advantages which cannot be obtained with currently available instruments. Such considerations prompted this study, which aims to develop an all solid-state, rapid-scanning multiwavelength thermal lens spectrometer that is stable and reliable and has the ability to simultaneously analyze multicomponent samples without any need for prior sample pretreatment. Preliminary results will be reported in this paper.

THEORY

Light is known to be diffracted by propagating sound waves. This is because an acoustic wave when propagated in a transparent material will produce a periodic modulation of the index of refraction (via the elasto-optical effect). This, in turn, will create a moving grating, which diffracts portions of an incident light beam. The diffraction process can, therefore, be considered as a transfer of energy and momentum. Conservation of the energy and momentum must, therefore, be maintained. The equation for conservation of momentum can be written as[12,13]

$$\vec{k}_d = \vec{k}_i \pm \vec{k}_s \tag{1}$$

where $\vec{k}_i$, $\vec{k}_d$, and $\vec{k}_s$ are the wave vectors of the incident and diffracted light and of the phonon. Depending on the optical properties of the medium where the acoustic interaction occurs, the diffraction processes can be divided into two categories: those in an optical isotropic medium where the polarization of the diffracted beam is the same as that of the incident beam and the anisotropic cases where the polarization of the diffracted beam is orthogonal to that of the incident beam.

In the first category, the acoustic interaction length is relatively short, the polarization of the incident and diffracted beams are the same, and the energy of the phonon is very small. Therefore, $|\vec{k}_d| = |\vec{k}_i|$, and the momentum matching triangle is isosceles. The incident and the diffracted angles are thus the same in this case ($\theta_i = \theta_d$) and have been shown to be related to the wavelength of the light λ and of the sound λ_s by the Bragg equation:

$$\sin\theta = |\vec{k}_s|/2|\vec{k}_d| = \lambda/2\lambda_s \tag{2}$$

This type of diffraction has been extensively used in such devices as acoustic-optic deflectors (i.e., Bragg cells) in which the diffraction angle of the light can be controlled by changing the frequency of the acoustic wave, namely, the change in the diffraction angle ($\Delta\theta$) is proportional to the change in the frequency of the acoustic wave (Δf_s) as $\Delta\theta = \lambda\Delta f_s/v_s$ (where v_s is the speed of sound).[20-23]

The acousto-optic tunable filter (AOTF) belongs to the second category in which acoustic interaction length is relatively long and the polarization of the diffracted light is orthogonal to that of the incident light. In this case the momenta of incident and diffracted photons are

$$|\vec{k}_i| = 2\pi n_i/\lambda \tag{3}$$

$$|\vec{k}_d| = 2\pi n_d/\lambda \tag{4}$$

and these are not equal since one is ordinary ray and the other is extraordinary ray (i.e., $n_i \neq n_d$). In the case of collinear AOTF, the incident and diffracted light beams and the acoustic beam are all collinear. If the incident light is an extraordinary ray and the diffracted light is an ordinary ray, the momentum matching condition becomes

$$\vec{k}_d = \vec{k}_i - \vec{k}_s \tag{5}$$

$$f_s = v_s(n_e - n_o)/\lambda \tag{6}$$

where $|\vec{k}_s| = 2\pi f_s/v_s$ and f_s and v_s are the frequency and velocity of the acoustic wave.

The collinearity requirement limits the filter materials to rather restricted classes of crystals.[12,13,24-26] For other crystals such as the paratellurite (TeO_2) used in this work, because of the symmetry, it is not possible to manufacture the collinear type AOTF. Noncollinear configuration AOTF has, in fact, been developed. It has been shown that eq 6 for the collinear AOTF can be generalized for the noncollinear AOTF

$$f_s = \frac{v_s(n_e - n_o)}{\lambda}(\sin^4\theta_i \sin^2 2\theta_i)^{1/2} \tag{7}$$

where θ_i is the incident polar angle. When $\theta_i = 90°$, eq 7 reduced to eq 6, i.e., the case of collinear AOTF.

It is thus evidently clear that in an anisotropic crystal where the phase-matching requirement is satisfied, diffraction occurs only under optimal conditions. These conditions are defined by the frequency of the acoustic waves and the wavelength of a particular diffracted light. For a given acoustic frequency, only light whose wavelength satisfies either eq 6 or eq 7 is diffracted from the crystal. The crystal can, therefore, be spectrally tuned by changing the frequency of the acoustic waves (i.e., f_s).

EXPERIMENTAL SECTION

A paratellurite (i.e., TeO_2) acousto-optic tunable filter was purchased from Matsushita Electronic Components Co., Ltd. (Kodama, Osaka, Japan, Model EFL-F20). This AOTF has a clear aperture of 3.0 × 5.0 min and is specified to have a resolution of 4 Å at 400 nm.[27] A voltage control oscillator (model DVCO-075A010) purchased from Inrad Northvale, NJ) was used to construct a driver for the AOTF.

The circuitry of the driver for the AOTF is shown in Figure 1. As illustrated, in this driver the pulse generator times the 3-bit programmable counter and gating circuit which addresses the eight-channel analog multiplexer (Maxim MAX 358). The multiplexer sequentially connects each of eight potentiometers

(17) Bates, B.; Halliwell, D. R.; McNoble, S.; Li, Y.; Catney, M. *Appl. Opt.* **1987**, *26*, 4783.
(18) Spring, K. R.; Smith, P. D. *J. Microsc. (Oxford)* **1987**, *147*, 265.
(19) Gottlieb, M.; Feichtner, J. D.; Conroy, J. *Proc. Soc. Photo-Opt. Instrum. Eng.* **1980**, *232*, 33.
(20) Yariv, A. *Optical Electronics*; 3rd ed.; Holt, Rinehart and Winston: New York, 1985.
(21) Skogerboe, K. J.; Yeung, E. S. *Anal. Chem.* **1986**, *58*, 1014.
(22) Huie, C. W.; Yeung, E. S. *Appl. Spectrosc.* **1986**, *40*, 863.
(23) Erskine, S. R.; Foley, C. M.; Bobbitt, D. R. *Appl. Spectrosc.* **1987**, *41*, 1189.
(24) Chang, I. C. *Appl. Phys. Lett.* **1974**, *25*, 370.
(25) Chang, I. C. *IEEE Trans. Sonics Ultrason.* **1976**, *23*, 2.
(26) Katzke, P. *Proc. SPIE: Int. Soc. Opt. Eng.* **1987**, *753*, 22.
(27) Operating Instructions for Model EFL-F20 Acousto-optic Tunable Filter. Matsushita Electronic Components Co., Ltd., Kodama, Osaka, Japan.

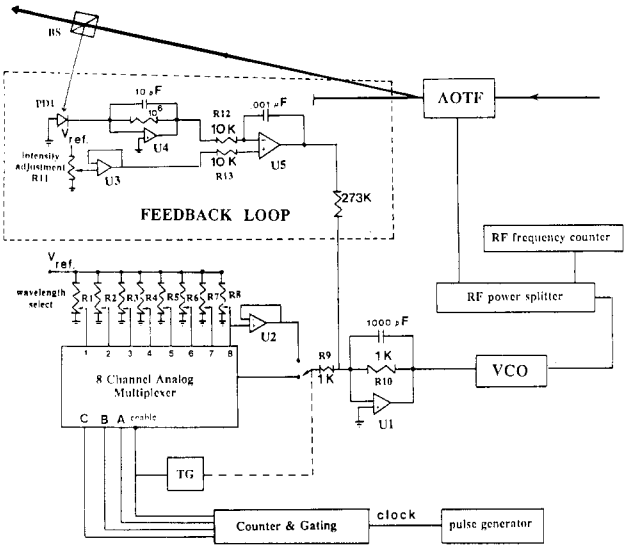

Figure 1. Circuit of the driver for the acousto-optic tunable filter.

to the control input of the voltage control oscillator (VCO) through a precision inverter. Each potentiometer is adjusted to provide a control voltage (V_{fc}) that will tune the VCO to the frequency required for the AOTF to diffract a specific wavelength. The frequency control voltage (i.e., V_{fc}) is a voltage in the range of 0.0–10.0 volt direct current (VDC) (i.e., 0.0 to −10.0 VDC after inversion) which is applied to the control input of the VCO. The VCO is adjusted to free run (i.e., V_{fc} = 0.0 VDC) at 80.000 MHz. It will provide a specific frequency when a voltage V_{fc} is applied into it. When operating in the "pulse" mode, the potentiometer of the channel number 8 is adjusted so that no light is diffracted by the AOTF. An analog transmission gate (TG, Maxim Model 333) alternatively selects either the output of the multiplexer (for the AOTF to diffract a specific wavelength) or the buffered output of the potentiometer number 8 (for the "dark" or no light to diffract from the filter).

As will be explained later, due to the time and temperature drift of the control voltage that tunes the VCO (to produce the required frequency) and of the VCO itself, it is very difficult to keep the frequency of the applied rf constant. As a consequence, intensities of light diffracted from the AOTF changed with time. A feedback loop (dashed line in Figure 1) was added to the driver to overcome this problem. As illustrated in the Figure 1, the beam diffracted from the AOTF was split by a beamsplitter to provide a reference beam for the feedback loop. In this loop, the output of the U5 integrator is an error voltage that represents the difference between the beam intensity at the monitor photodiode and the desired intensity as set by the intensity adjustment switch (R11). A balance condition is achieved when the error voltage is zero; a negative value indicates that the intensity at the monitoring photodiode is greater than the set intensity and vice versa. The loop is closed by summing the output of the error voltage and the wavelength select multiplexer. Initially, the applied rf frequencies were selected to place the diffracted beams on the negative slopes of the bands. As a consequence, any increase in the frequency of the VCO will result in the decrease in the intensity of the diffracted beams. The feedback is operated because any increase in the intensity at the monitoring photodiode will result in the increase in the frequency of the VCO and hence the decrease in the intensity of the diffracted beam. As a consequence the diffracted beam intensity remains the same.

RESULTS AND DISCUSSION

1. Characteristics of the TeO_2 Acousto-Optic Tunable Filter. A Spectra-Physics Model 165 argon ion laser was used as the light source. It provided a multiline laser beam which was a mixture of six different wavelengths: 514.5, 501.7, 496.5, 488.0, 476.5, and 457.9 nm. It was found that monochromatic laser light having a spcific wavelength was diffracted from the AOTF when the filter was incident by this multiline beam and applied by an appropriate rf frequency. As an example, when a frequency of 75.8522 MHz was applied to the filter, only the 457.9-nm light was diffracted from the filter. Relatively lower frequencies were needed for longer wavelengths. For instance, 71.5820, 69.1730, 67.5232, 66.5643, and 64.3115 MHz were found to be the frequencies required to diffract light having wavelengths of 476.5, 488.0, 496.5, 501.7, and 514.5 nm, respectively.

The relative intensity of the light diffracted from the AOTF as the function of the applied rf frequency is shown in Figure 2. As illustrated, for each wavelength in addition to the main bands there are several small side bands. It is important to point out that side bands and the main band have the same spectral purity, i.e., they have exactly the same wavelength. The side bands (or side lobes) which are often seen in AOTF[11-13,17,18,24-26] are produced by the mismatch between the spreading of the acoustic beam from a source of finite size and the width of the central peak, which is largely determined by the limited interaction length. Specifically, the profile of the spectral band pass is the square of the Fourier transform of the acoustic profile along the light path. The filter function is, therefore, a sinc^2 response. Several methods can be used to depress these side bands. For instance, it was found by other workers and by us that appropriately adjusting the power of the applied rf may provide substantial reduction of the side bands.[17,28] For this particular TeO_2 AOTF we found that the diffraction efficiency (and hence the intensity of the diffracted light) is proportional to the power of the applied rf.[28] The proportional constants are, however, different for the main band and the side bands. Appropriate selection of the power will, therefore, lead to a substantial reduction of the side bands. As an example, for the 488.0-nm light, at 10 mW applied rf signal, the ratio of the main band to the first side ban is 9.0; increased the rf power to 35 mW, which is the optimal power for maximum diffraction efficiency (for the main band), increased the main band but also increased the side bands as well.[28] Since the side bands increase more than the main band in this region, the ratio of the main band to the first side band decreased to 4.5.[28] Alternatively reduction of the side bands can also be achieved by apodizing the acoustic profile.[11-13,17,18,24-26,29] It has been reported that by use of the apodization method based on the Hamming window, the first side bands were reduced 30 dB (i.e., 10^3) below the main band.[29]

It is noteworthy to add that in the present work because a multiline laser is used as the light source, the side bands have the same spectral purity as the main bands. As a consequence, their presence does not degrade the resolution but rather adds additional advantage to the AOTF. This is because, as shown in Figure 2, the relative intensity of the diffracted light of the main band is very different from one wavelength to another, e.g., the intensity of the diffracted 488.0-nm main band is 23 times that of the 457.9-nm main band. According to this intensity–frequency relationship, intensity of all diffracted beams can be adjusted to be equal when the frequency corresponding to side bands of the higher intensity beams and the frequency corresponding to the main bands of the lower beams are used together.

In addition to the dispersion and scanning ability, the AOTF can also serve as an electronic shutter for the amplitude modulation of the diffracted beam. This capability stems from the fact that the wavelength of the diffracted light is dependent on the frequency of the applied rf. No light will be diffracted out of the AOTF when the applied frequency

(28) Tran, C. D.; Furlan, R. J., unpublished work.
(29) Chang, I. C.; Katzka, P. *J. Opt. Soc. Am.* **1978**, *68*, 1449.

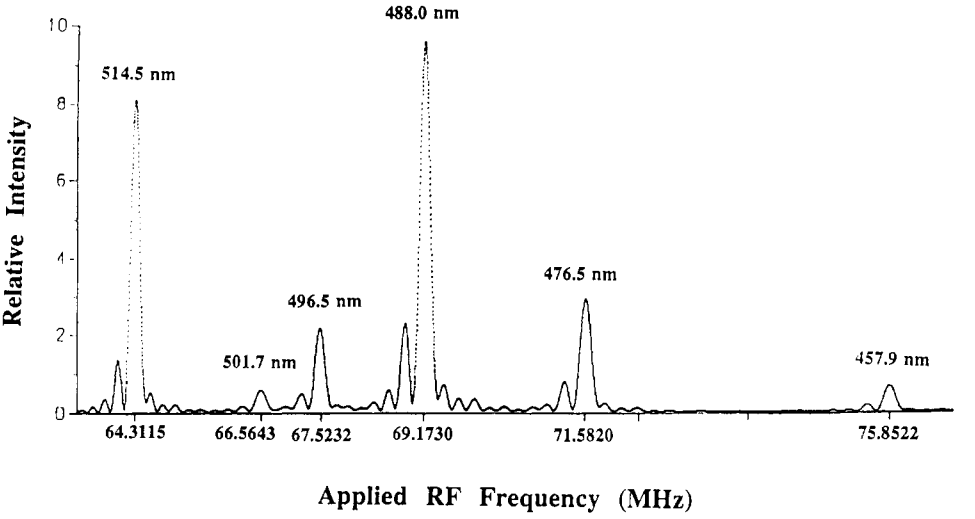

Figure 2. Spectral profile of the light diffracted from the acousto-optic tunable filter as a function of the frequency of the applied rf.

does not correspond to any wavelengths in the input beam. Therefore, by controlling the frequency, duration, and scanning speed of the applied rf, the spectral scanning and amplitude modulation of the diffracted light can be readily achieved. In this operation, the AOTF driver is used in the so-called "pulse" mode. Results obtained (without the feedback loop and with a neutral density filter in front of the photodiode to prevent it from saturation) are plotted as the intensity of the diffracted beams as a function of time as shown in Figure 3a. As illustrated by sequentially varying the frequency of the applied rf from f_1, f_8, f_2, f_8, f_3, f_8, f_4, f_8, f_5, f_8, f_6, f_8 (where f_1 = 64.3115, f_2 = 66.5643, f_3 = 67.5232, f_4 = 69.1730, f_5 = 71.5820, f_6 = 75.8522, and f_8 = 80.0000 MHz), the incident multiline laser beam was not only sequentially diffracted as monochromatic beams having wavelengths 514.5, 501.7, 496.5, 488.0, 476.5, and 457.9 nm but also following each diffracted beam there was always a dark period where no light was diffracted out of the AOTF. This is because during these dark periods the AOTF was applied by f_8 = 80.0000 MHz, which does not correspond to any wavelength in the incident beam. Of course by omitting the applied frequency f_8, the AOTF can be made to switch from one wavelength to the next without any dark period.

There are substantial differences in the intensities of diffracted beams shown in Figure 3a. The differences arise because the applied frequencies f_1, f_2, f_3, f_4, f_5, and f_6 correspond to the peak of the highest band for each wavelength. As explained earlier, this inequality can be eliminated by appropriately selecting the frequency of the applied rf and by activating the feedback loop of the driver. Figure 3b showed the results obtained without the feedback loop and the neutral density filter. The applied frequencies for higher intensity beams (i.e., 514.5, 496.5, 488.0, and 476.5 nm) were set at either a smaller band or the side of the band. As illustrated, the relative intensities for the diffracted beams are very close but not exactly equal. This is because, in this case, the feedback was not activated and it was difficult to manually set the exact frequencies for the applied rf in the side-band regions where the slope is very large. Furthermore, it was not possible to keep the beam intensity at a constant level over a period of time. The variation in the beam intensity as a function of time can be due to a variety of factors including the fluctuation in the intensity of the laser, the change in the efficiency of the AOTF, and the change in the frequency of the rf supplied by the voltage control oscillator (VCO). The temperature effect on the efficiency of the AOTF is known to be very small. Since, in the present work, the power of the applied rf was on the order of 20 mW, the heat generated by this rf is expectedly very small. Consequently, it is anticipated that the fluctuation in the intensity of the diffracted beams is due mainly to the instability of the laser and to the changes in the frequency of the applied rf. The time and temperature drift of the control voltage that tunes the VCO to produce the required frequency, and of the VCO itself, are responsible for the change in the applied rf frequency. It is estimated that for the 488.0-nm diffracted beam, the fluctuation of 0.20% in the applied voltage will produce a change of 3.7 mW in the intensity of the diffracted beam. While it is true that this estimation illustrates the worst case since it was calculated for the largest slope of the highest intensity beam, it is evident that the fluctuation in the intensity of the diffracted beam is so large that it is difficult to use the AOTF in any type of quantitative instruments such as the thermal lens spectrometer without the feedback mechanism.

Figure 3c showed results obtained when the AOTF was driven by the driver with its feedback mechanism is operation. Compared to the previous case (i.e., Figure 3b), the feedback system provides the needed corrections to compensate for the fluctuation and differences in the intensities of the diffracted beams. As depicted in the Figure 3c, the intensity of the diffracted beam for six different wavelengths was maintained by this feedback loop to be exactly the same.

Collectively, the results presented clearly demonstrate that the AOTF can successfully and uniquely serve as an all solid-state, nonmoving parts dispersive device to quickly scan and keep the amplitude of the diffracted light constant. The AOTF used in this study was fabricated from TeO_2 so that it can only be used for wavelengths longer than 360 nm. The recently developed quartz AOTF extends the use of the filter to wavelengths as low as 240 nm.[30] Furthermore, in this study, a laser was used as the light source. However, since the AOTF has a relatively large acceptance angle (as compared to the conventional acousto-optic deflectors based on Bragg cells), it can be utilized for other light sources which do not provide low diverging, well-collimated beams, e.g., incandescent and arc lamps. It should be noted that, for such continuous light sources, side bands of one color may overlap with those of other color and, hence, degrade the resolution of the filter. Experiments are now in progress to use AOTF in combination with continuous light sources and to depress the side bands by either controlling the power of the applied rf and/or apodization. In the present work the AOTF was used to construct the first multiwavelength thermal lens spectropho-

(30) Katzka, P.; Chang, I. C. *Proc. Soc. Photo-Opt. Instrum. Eng.* **1979**, *202*, 753.

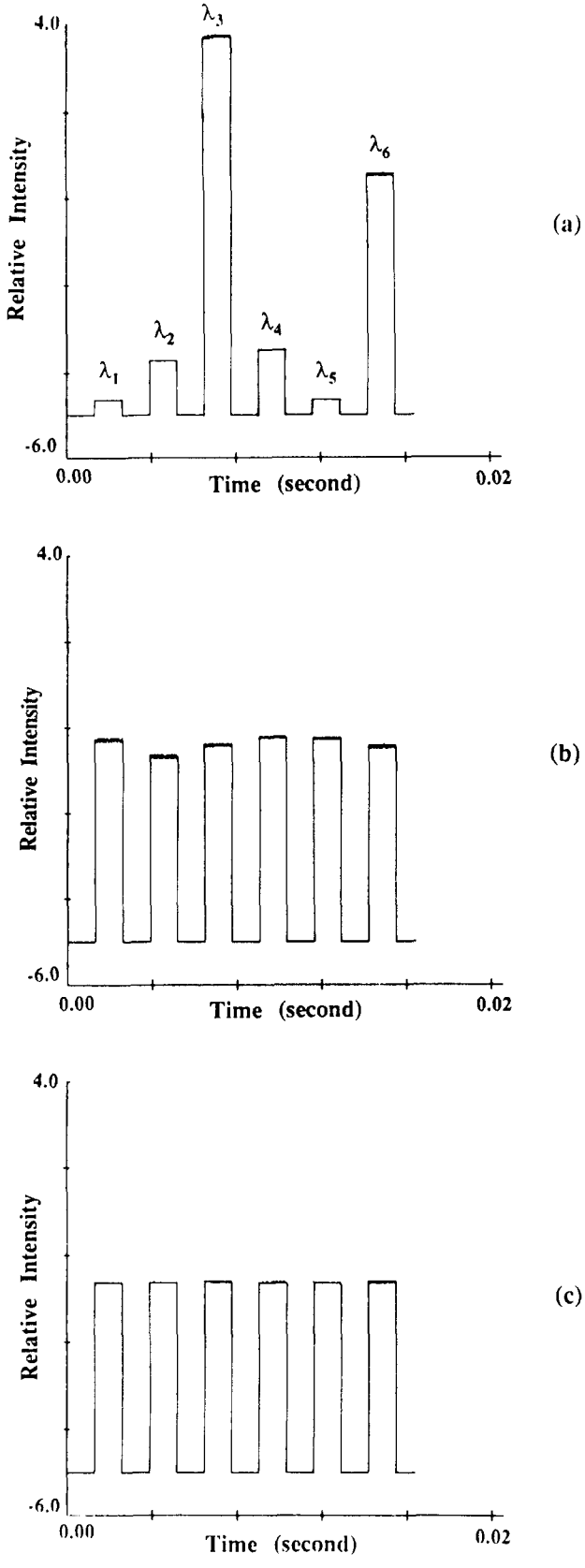

Figure 3. Relative intensity of six different wavelength laser beams diffracted and modulated by the acousto-optic tunable filter; λ_1 = 501.7, λ_2 = 496.5, λ_3 = 488.0, λ_4 = 476.5, λ_5 = 457.9, and λ_6 = 514.5 nm. (a) Frequencies of the applied rf correspond to the peak of bands shown in Figure 2. (b) Frequencies of the applied rf correspond to the side of bands, with the feedback loop off. (c) Same as in (b) but with the feedback loop on. See text for detailed information.

tometer. The instrumentation development and preliminary results will be described in the following section.

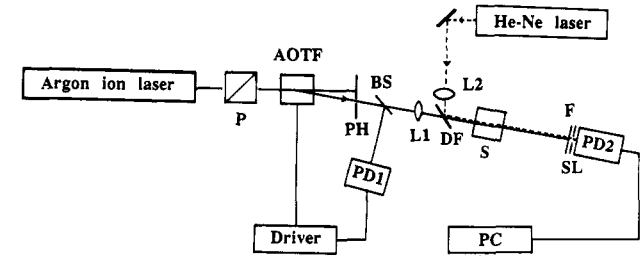

Figure 4. Schematic diagram of the AOTF-based multiwavelength thermal lens spectrophotometer: P, polarizer; AOTF, acousto-optic tunable filter; PH, pinhole; BS, beam splitter; L1, achromatic spherical lens; DF, dichroic filter; L2, cylindrical lens; S, sample; F, interference filter; SL, slit; PD1 and PD2, PIN photodiodes.

2. Multiwavelength Thermal Lens Spectrophotometer Based on AOTF. The schematic diagram of the AOTF-based thermal lens spectrophotometer is shown in Figure 4. As shown in the Figure 4, in this instrument, the Spectra-Physics Model 165 argon ion laser, operated in the multiline mode, was used as the excitation source. The laser beam was converted to completely vertically polarized by means of a Glan-Thompson prism polarizer. The TeO_2 noncollinear AOTF was used to select the appropriate wavelength from the multiline incident laser beam, to provide the amplitude modulation of the diffracted beams, and to scan from one wavelength to another. A small part of the diffracted beam was split into the reference photodiode (PD1) by means of a beam splitter. The output of this photodiode provided the reference for the feedback loop of the AOTF driver. The diffracted beam, which was transmitted through the reference beam splitter, was focused onto the sample by a 100-mm achromatic lens. The probe beam, provided by a He–Ne laser (Spectra-Physics Model 105), was aligned to overlap with the pump beam at the sample cell by means of a dichroic filter (DF). The heat generated by the sample absorption of the pump beams changes the intensity of the probe beam. The intensity fluctuation of the probe beam was measured by a PIN photodiode (PD2) placed behind a 632.8-nm interference filter (F) and a slit (S). A 50-mm focal length cylindrical lens was used to focus the probe beam into a thin line. The distance between the lens and the sample was adjusted to give maximum thermal lens signals. The signal intensity was measured as the relative change in the probe beam center intensity. This was accomplished by use of a PC through a MetraByte DAS 18 AD board.

Generally, in conventional thermal lens instruments, the probe beam is focused by a spherical lens and a pin hole is used to facilitate the detection of the probe beam center intensity. Conversely, in the present multiwavelength thermal lens spectrophotometer, a cylindrical lens and a slit were used instead. This modification was made to eliminate the aberration induced by the chromaticity of the AOTF. The chromaticity stems from the relatively high refractive index of the TeO_2 (n = 2.26).[16] We have investigated this deviation by measuring the diffracted angle, which is defined as the angle between the transmitted and diffracted beams, for each wavelength. Results obtained, listed in Table I, clearly indicate that there are slight differences in the diffraction angles for the range of wavelengths used (i.e., 457.9 and 514.5 nm). Within this range, the largest difference was found to be 1.35%, and that is for the difference between the lowest and highest wavelengths. While this value seems rather small, it produces error when thermal lens signals for difference excitation wavelengths were compared. The error is produced because the thermal lens signal intensity is known to be proportional to the overlap in the sample between the excitation and the monitoring beams. Due to the difference in the diffraction angles, the overlap between the two beams

Table I. Properties of TeO_2 Acousto-Optic Tunable Filter

wavelength, nm	applied frequency, MHz	relative intensity,[a] mW	diffracted angle,[b] deg
457.9	75.8522	5.0	2.995 ± 0.008
476.5	71.5820	19.0	3.01 ± 0.01
488.0	69.1730	115.0	3.02 ± 0.01
496.5	67.5232	16.2	3.02 ± 0.01
501.7	66.5643	4.6	3.03 ± 0.01
514.5	64.3115	95.0	3.04 ± 0.01

[a] A 295-mW multiline laser beam from an argon ion laser was used as the incident beam. [b] Angle between the transmitted and diffracted beam.

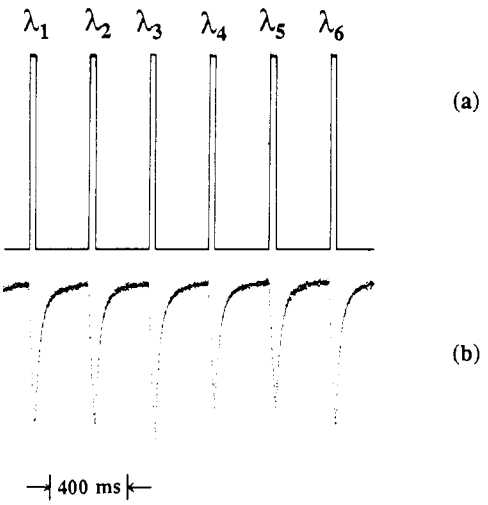

Figure 5. Excitation beam intensity and probe beam intensity as a function of time: (a) excitation beam intensity for the λ_1 = 501.7, λ_2 = 496.5, λ_3 = 488.0, λ_4 = 476.5, λ_5 = 457.9, and λ_6 = 514.5 nm; (b) probe beam intensity measured by using the six excitation beams shown in (a) on a sample of 2.2×10^{-7} M ferroin in methanol.

is not the same for different excitation wavelengths. We have undertaken two approaches to overcome this problem: (1) use of a cylindrical lens and a slit instead of a conventional spherical lens and a pin hole and (2) special alignment of the system. The AOTF was aligned to diffract all (excitation) wavelengths in the same vertical plane. The probe beam was focused to a vertical line overlapping with the (excitation) vertical plane by means of a cylindrical lens. The slit was aligned in such as way that it is parallel to the focus line of the probe beam (and hence, the vertical plane of the excitation beams as well). We found that this arrangement did, in fact, provide the compensation for aberration due to the chromaticity of the AOTF. This is because the pump beam, even when it was deviated by the chromaticity of the AOTF, was still in the same vertical plane and, thus, was within the focused line of the probe beam. As a consequence, the overlap between the two beams remains the same for all excitation wavelengths. Intensity of the probe beam is changed as a consequence of the sample absorption of the pump beam, and this fluctuation is spatially different in the horizontal plane but not the vertical plane. Since the photodiode detects the fluctuation in the probe beam intensity behind a slit parallel to the vertical lens, any change in the horizontal plane by the chromaticity of the AOTF will not have any contribution to the measured thermal lens signals.

The intensity profiles of the excitation beams and the probe beam, obtained with the use of this AOTF-based multiwavelength thermal lens spectrophotometer, are shown in Figure 5. The sample was sequentially excited by six different excitation wavelengths, i.e., 514.5, 501.7, 496.5, 488.0, 476.5, and 457.9 nm, whose intensities as measured by the reference

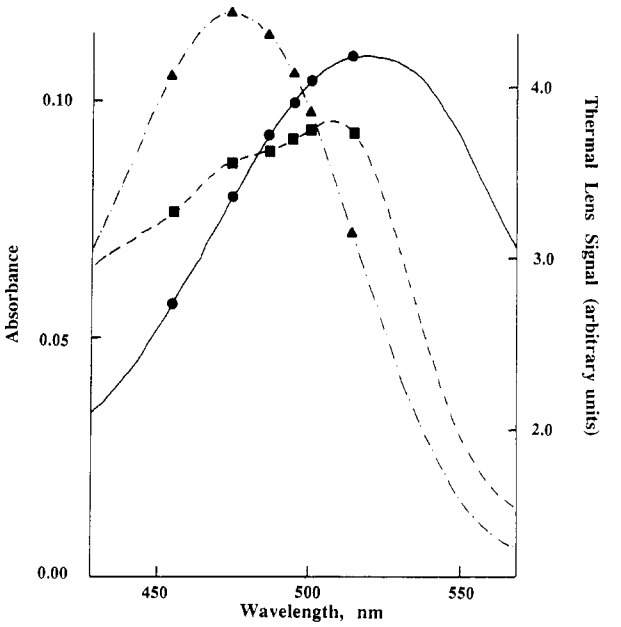

Figure 6. Absorption spectra (lines) and thermal lens signals (shapes) of 1,2-diaminoanthraquinone (— and ●), 1-amino-8-chloroanthraquinone (– • – and ▲) and 1,10-phenanthroline–iron(II) (– – and ■).

photodiode (PD1) are shown in Figure 5a. As shown, intensities of six beams as detected by the PD1 were exactly the same and remained the same as long as the feedback loop is engaged. It is important to point out that the same intensity detected by this PD1 reference photodiode does not necessarily mean that the intensity of six (different wavelength) excitation beams at the sample is the same. In fact, their intensities were found to be different. The differences stem from the spectral response of the reference photodiode and the chromaticity of the beam splitter (BS) and the dichroic filter (DF). Accordingly, a power meter was placed at the sample to measure the exact intensities of six beams excited in the sample, and the values obtained were then used to calculate the exact intensities of excitation beams (from the values measured by the reference photodiode PD1) and to normalized the thermal lens signal. It should be added that even though intensities of excitation beams at the sample are not equal, they remain the same at those levels as long as the feedback loop is employed. Effort is now concentrated in incorporating the calibration factors to the feedback mechanism so that the intensity of excitation beams at the sample is the same.

As depicted in Figure 5a, between two consecutive excitations, there was always a dark period in which the sample was not excited by any beams. This dark period enabled the sample to return to its original thermal state before being excited again. To ensure that the sample had adequate time to relax, the dark period was set to be 9 times longer than the open period. The heat generated as a consequence of the absorption of the excitation beams by the sample [2.2×10^{-7} M of 1,10-phenanthroline–iron(II) perchlorate (ferroin) in methanol] was monitored by the probe beam, whose beam center intensity as recorded by the photodiode (PD2) is shown in Figure 5b. As depicted, the intensity of the probe beam decreased when the excitation beam was on because the heat that was generated by the sample absorption produced a diverged thermal lens to defocus the probe beam. As a consequence, the probe beam center intensity is decreased.

The thermal lens signals were normalized by dividing the peak height of the probe beam (eg., Figure 5b) by the corresponding excitation beam intensities at the sample. For comparison, results obtained for ferroin, 1,2-diaminoan-

thraquinone (DAA), and 1-amino-8-chloroanthraquinone (ACA) were plotted in Figure 6 together with their absorption spectra measured by using conventional transmission instrument. As expected, the thermal lens results agree well with the sample absorption spectra. It is thus evidently clear that the multiwavelength thermal lens technique can provide fingerprints and, hence, information on the identity of sample. On the basis of the preliminary results, the limit of detection (LOD), defined as the concentration of the sample that yielded a signal-to-noise ratio of 2, was estimated to be 1.0×10^{-10} M for 1,2-diaminoanthraquinone in methanol. This LOD value is comparable to other LOD values found on other thermal lens instruments.[4-10] Experiments are now in progress to use the developed instrument for the characterization of trace chemicals and for the analysis of a sample having as many as six different components.

Taken together, these results clearly demonstrate that an all solid-state, nonmoving parts, fast-scanning multiwavelength thermal lens spectrophotometer can be successfully constructed using the acousto-optic tunable filter. The spectrophotometer not only provides fingerprints of analytes but also can be used for the analysis of multicomponent samples. Due to the limited number of wavelengths of the argon ion laser used in this work, the present spectrophotometer can only be used to analyze sample having up to six different components. Since the tuning range of the AOTF is from the UV through visible through IR, a truly multiwavelength (i.e., white light) thermal lens spectrophotometer can, in principle, be constructed using a combination of lasers. Such an instrument will expand the application of the thermal lens technique to the area of general trace analyses for real-time samples. Experiments are now in progress to explore this possibility.

ACKNOWLEDGMENT

We are indebted to Mark Bartelt and Ricardo Furlan for their competent technical assistance. Acknowledgment is made to the National Institutes of Health, National Center for Research Resources, Biomedical Research Technology Program for financial support of this work.

RECEIVED for review January 31, 1992. Accepted April 13, 1992.

Registry No. DAA, 1758-68-5; ACA, 117-09-9; ferroin, 14708-99-7.